WIDEBAND MONOPOLE ANTENNA AND METHODS TO ENHANCE ITS PERFORMANCE

Tho Ching Shuen Shannon[1], Lim Zi Wei[2], Ang Teng Wah[2],
[1]Hwa Chong Institution (College), 661 Bukit Timah Rd, Singapore 269734
[2]DSO National Laboratories, 12 Science Park Drive Singapore 118225

ABSTRACT
Conventional quarter-wave monopole antennas ($\lambda_o/4$) often suffer from narrow bandwidth and high profile. This project aims to study methods to enhance the monopole antenna's bandwidth while offering a height as short as possible. A novel antenna with a low profile of 16mm ($0.12\lambda_o$ at 2.3GHz) is proposed, consisting of a conical monopole with a shorted ring patch. The simple monocone was designed to suit a higher frequency band, while the shorted ring patch was adopted to generate additional lower frequency bands, resulting in a design with a wide 10dB return loss bandwidth of 15.8GHz (2.2-18.0GHz). The fabricated antenna provides broadband characteristics and is suitable for UWB, WiBro, WLAN, DMB, and various other wireless services. This paper discusses the design, fabrication and operating characteristics of the proposed antenna.

INTRODUCTION
Due to the recent demand for modern broadband communication services, the monopole antenna has received much attention due to its attractive advantages such as simplicity, light weight and easy fabrication [1–6]. The monopole antenna is commonly used to provide omnidirectional transmission and reception of microwave signals.

However, conventional monopole antennas can only operate efficiently within a narrow bandwidth due to their omnidirectional characteristics. Thus, tiny disturbances in frequency due to environmental change will seriously affect their operational behaviour. Moreover, antennas for vehicle-mounted devices and indoor wireless networks require a low profile [7, 8], putting stringent requirements on an antenna's physical size [9, 10]. The height of a conventional quarter wavelength monopole ($\lambda_o/4$) is often too large for conformal devices.

This project aims to study methods to enhance the monopole antenna's bandwidth while offering a height as short as possible.

HYPOTHESIS
This project will result in the conception of an antenna of height less than one-eighth of the free-space wavelength associated with its lowest operating frequency ($\lambda_o/8$), and able to fully cover the ultra-wideband (UWB) frequency range of 3.1-10.6GHz.

MATERIALS AND METHODS
The main objectives of this project are summarised below:

1. Conduct an investigation into the optimisation of the monopole antenna design using various three-dimensional (3D) shapes.
2. Propose an innovative monopole antenna design using novel techniques.
3. The proposed antenna is to be fabricated and tested to verify the simulation result.

A parametric study of the monopole antenna was carried out using Ansys HFSS, to analyse the return loss characteristics of the proposed designs. Varying the antenna's geometrical dimensions allows one to centre the resonance in the middle of the required bandwidth, achieving the optimal design. After which, a prototype antenna is fabricated based on the collected results. The antenna's performance is measured using a Vector Network Analyser (VNA).

RESULTS

1. *Optimisation of Antenna Shape*

Monopoles of various 3D shapes were simulated on a square ground plane of 100mm × 100mm, fed by a coaxial cable at the centre. The height of the structure was limited to 37.5mm, ⅛ of the wavelength associated with the lowest operating frequency of 1GHz. This project focuses on techniques to match the monopole antenna to a desired characteristic impedance of 50Ω. In simulation, the -15dB reflection coefficient bandwidth was measured instead of -10dB, to account for any degradation in the performance of the antenna in the process of fabrication.

Fig. 1: For the monopole: (a) Geometry, (b) Simulated return loss for h *4-7mm, and (c) Simulated return loss for* r *1-4mm.*

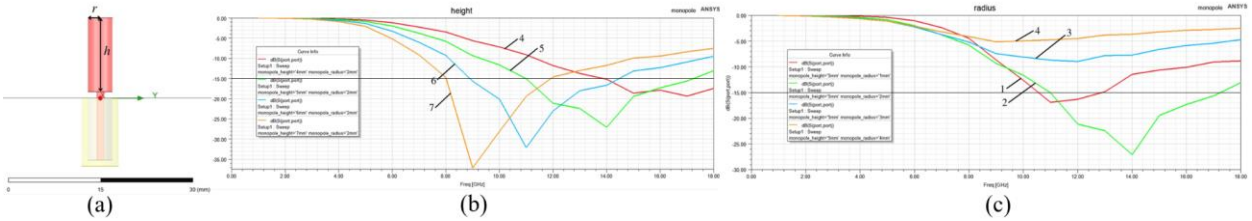

(a) (b) (c)

In Fig. 1(b), as the monopole's height (*h*) increases, the resonant point shifts to a lower frequency. However, beyond *h*=5mm, the 15dB return loss bandwidth narrows and impedance matching deteriorates. As shown in Fig. 1(c), the optimal monopole design is of *h*=5mm and radius *r*=2mm, giving a 6.2GHz 15dB return loss bandwidth (11.0-17.2GHz).

Fig. 2: For the cuboid: (a) Geometry, (b) Simulated return loss for l *2-4mm, and (c) Simulated return loss for* h *1-10mm.*

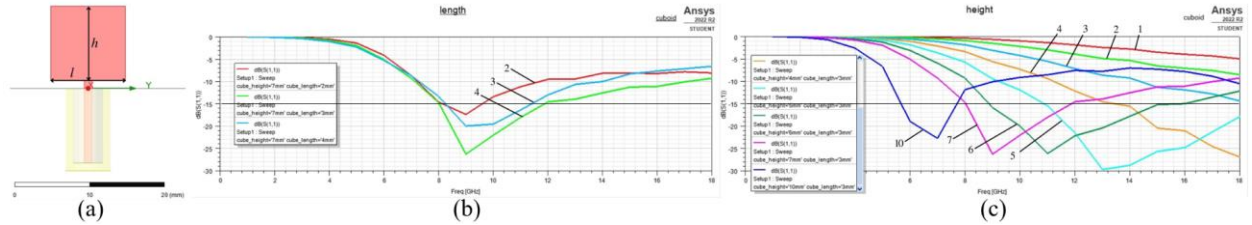

(a) (b) (c)

In Fig. 3(b), 3mm is the optimal length (*l*) of the square base. As seen in Fig. 3(c), as its height (*h*) increases, the resonant point shifts to a lower frequency and impedance matching improves. However, beyond *h*=6mm, the 15dB return loss bandwidth narrows. As such, the optimal dimensions are *l*=3mm and *h*=6mm, yielding a 6.2GHz return loss bandwidth (8.8-15.0GHz).

Fig. 3: For the monocone: (a) Geometry, (b) Simulated return loss for lr *1-3mm, (c) Simulated return loss for* ur *11-15mm, and (d) Simulated return loss for* h *14-18mm.*

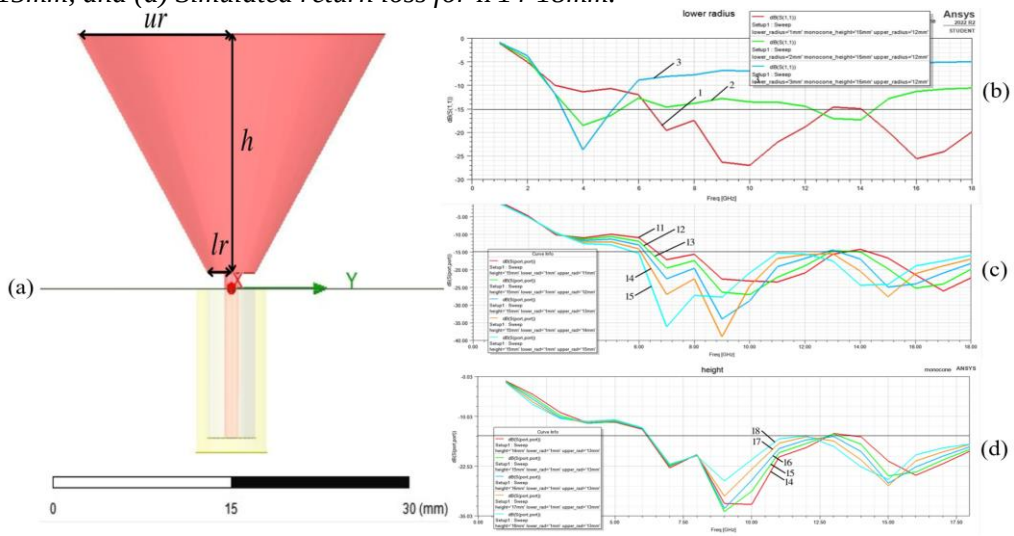

It can be observed in Fig. 3(b)-(c) that the effect of varying the lower radius (*lr)* is more significant than that of the upper radius (*ur)*. A combination of *lr*=1mm and *ur*=14mm yields the best results. In general, increasing the flare angle of the antenna by increasing *ur* and decreasing *lr* results in a downward shift of the resonant point, improving impedance match. Using the optimised values of *ur* and *lr*, the monocone functions best at a height (*h*) of 16mm as shown in Fig. 2(c), yielding a 11.9GHz return loss bandwidth (6.1-18.0GHz).

Fig. 4: For the sphere: (a) Geometry, and (b) Simulated return loss for r *3-6mm.*

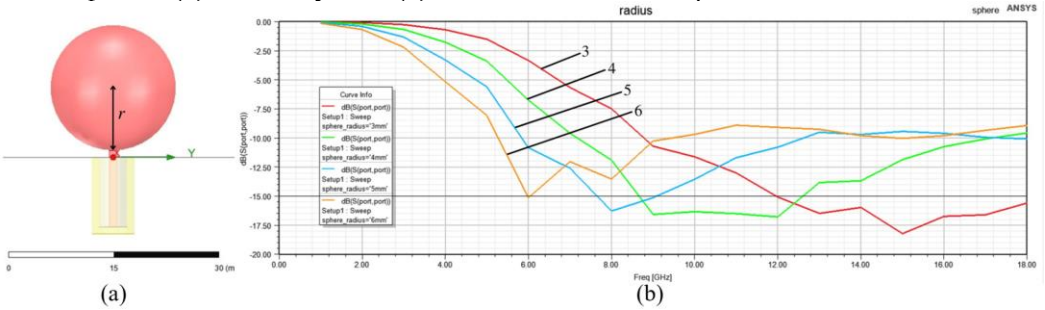

In Fig. 4 (b), the optimal sphere radius *r*=3mm, giving a 6.0GHz return loss bandwidth (12.0-18.0GHz). As *r* increases, the 15dB return loss bandwidth narrows and the resonant point shifts upward, hence the impedance matching deteriorates.

Generally, varying the height of the antenna has the most profound effect on its performance. Increasing the height usually quickly shifts the resonant point toward lower frequencies, enhancing the lower-band impedance matching. However, increasing height also often narrows the 15dB return loss bandwidth at higher frequency bands.

Table 1: Impedance bandwidth of the optimised antenna design for each 3D shape.

Shape	**Bandwidth (GHz)**	**Range (GHz)**
Monopole	6.2	11.0-17.2
Cuboid	6.2	8.8-15.0
Monocone	11.9	6.1-18.0
Sphere	6.0	12.0-18.0

As seen in Table 1, using different 3D shapes of antennas helps achieve modified bandwidth. In particular, with the monocone structure, a significant improvement on the bandwidth by up to 91.9% can be achieved as compared to the simple monopole. The monocone significantly improves impedance at lower-band frequencies. The resultant design will be labelled as Ant. 1: *lr*=1mm, *ur*=14mm, *h*=16mm on a square ground plane of length 100mm.

2. *Additional Design Elements*

Fig. 5: (a) 3D view of the proposed antenna design, and (b)-(c) Geometry of the design.

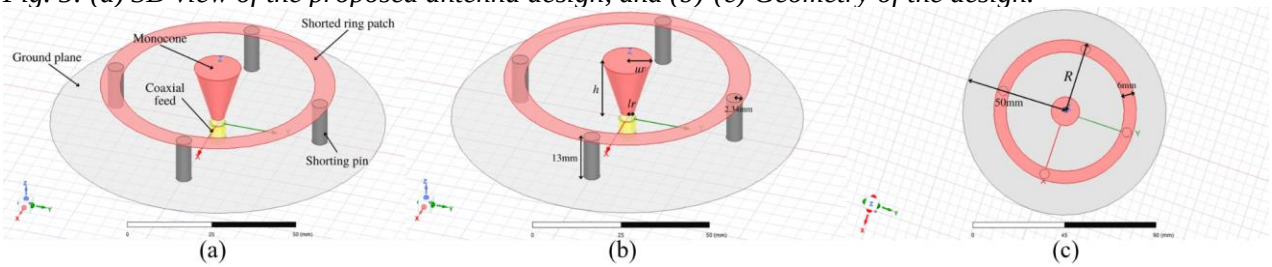

To fulfil the requirements of a low profile and wide bandwidth, the proposed antenna as seen in Fig. 5(a) consists of a monocone antenna with a circular ring patch shorted to a circular ground plane using four shorting pins, inspired by [11] which proposed incorporating the circular patch antenna with the traditional monopole antenna. The next section aims to investigate and validate the potential improvements in the previously proposed design.

Four shorting pins of radius 2.34mm and height 13mm are positioned at the centre of the ring patch of width 6mm and variable radius *R*. The pins are symmetrically located from the centre of the feed point and connected to a circular ground plane of radius 50mm. The following section investigates the effects of varying the ring patch radius and the dimensions of the monocone, which are parameters that have been verified from simulation to have a more significant effect on antenna performance as compared to the variables that have been fixed as above[1].

1 *Simulated return loss characteristics of varying other variables found in Appendix Fig. 10.*

Fig. 6: Simulated return loss for (a) R *25-40mm with 5mm step size, and (b)* h *15-20mm.*

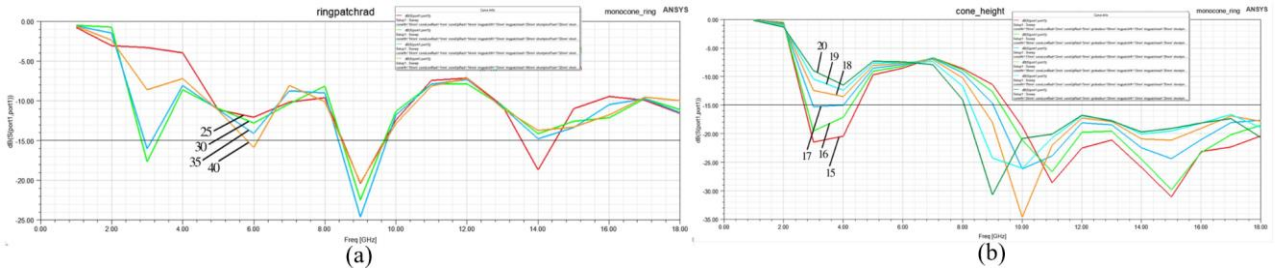

As seen in Fig. 6(a), as the radius of the ring patch (*R*) increases, impedance matching improves due to the addition of another resonant mode in the low frequency range. However, after *R*=35mm, the resonant point shifts upward and the effect is reduced. *R* is selected as 35mm.

The *lr* and *ur* of the cone were then optimised using similar techniques as used above[2], giving *lr*=2mm and *ur*=5mm. In Fig. 6(b), with a decrease in height of the cone (*h*), an additional resonant mode is achieved at the low frequency range, extending the lower band frequency limit. However, the bandwidth at the higher frequency band is partially compromised by increasing *h*. The case of *h*=16mm, *ur*=7mm and *lr*=2mm provides the optimal design, in which there are two resonant modes without significantly affecting the higher-band impedance characteristic. This design, Ant. 2, has a return loss bandwidth of 10.3GHz (2.8-4.3GHz and 9.2-18.0GHz).

Although the bandwidth of the higher frequency band is partially reduced by adding the shorted ring patch, the ring patch expands the antenna bandwidth at the low frequency limit. Moreover, the gradient variation on the surface of the monocone helps improve the impedance matching at the high frequency band. Consequently, the antenna has two operating bands instead of one.

3. *Antenna Fabrication and Measurement*

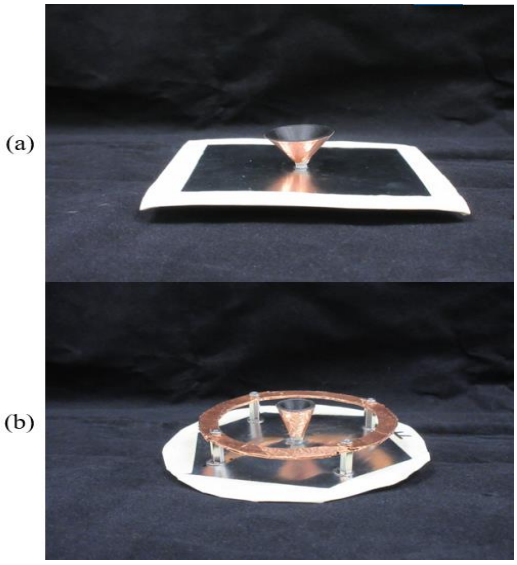

Fig. 7: Photographs of the fabricated antennas: (a) Ant. 1 (b) Ant. 2.

Prototypes of Ant. 1 and 2 (Fig. 7) were fabricated. The monocones and ring patches were 3D-printed using carbon fibre, then lined with copper tape of thickness 0.07mm. The ground planes are made from aluminium of thickness 0.30mm, and the shorting pins are made of steel. To coaxially feed the antenna, the SubMiniature version A (SMA) connector was soldered. The feeding coaxial cable has a 50Ω characteristic impedance.

2 *Simulated return loss characteristics of varying* lr *and* ur *found in Appendix Fig. 11.*

Fig. 8: Simulated (red) and measured (blue) return loss plots for (a) Ant. 1 (b) Ant. 2.

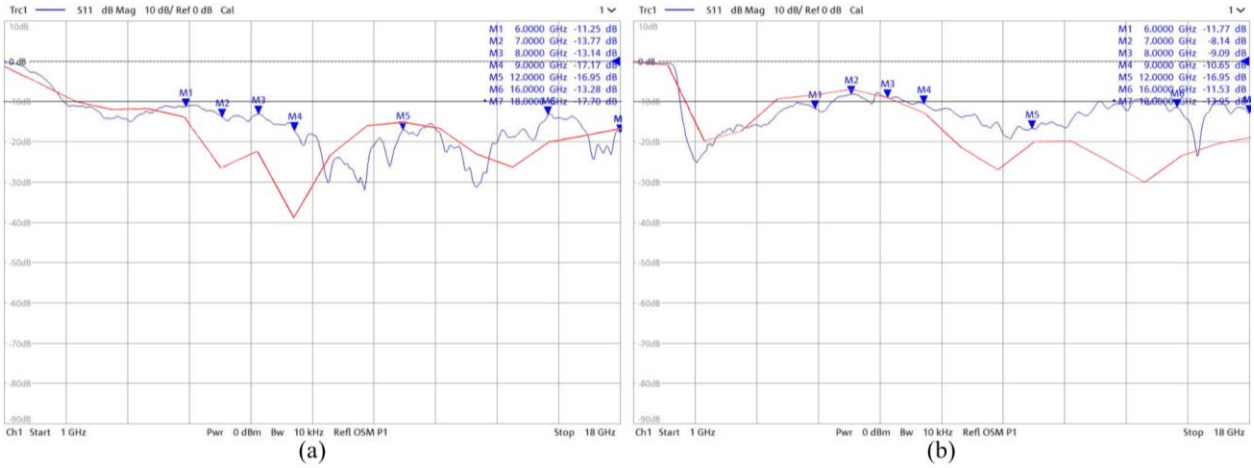

The VNA was used to measure the return loss at each port of the fabricated antenna. Although the simulated and measured results (Fig. 8) are in relatively good agreement, with the general trends of each graph in good match, the measured structure presents slight frequency shifts. This implies a narrower -15dB reflection coefficient bandwidth in measurement than in simulation. Taking roughly 10dB instead as the required return loss, the measured impedance bandwidths are 15.3GHz (2.7-18.0GHz) and 15.8GHz (2.2-18.0GHz) for Ant. 1 and 2 respectively.

DISCUSSION

The results clearly indicate that the shorted ring patch can significantly improve the impedance matching at lower frequencies. By an optimised choice of the dimensions of the elements involved, both the simulated and measured results have shown that it is possible to induce a wide frequency band using the proposed design of Ant. 2.

By shorting the ring patch to the ground plane, the low frequency limit is expanded due to the additional mode generated at the frequency below the fundamental mode [12]. Resonance is generated by the anti-resonance formed by a parallel circuit containing the capacitance between the ring patch and ground plane, and the inductance of the shorting pins. Since electromagnetic fields at higher frequencies diffract from regions closer to the feed and those at lower frequencies diffract from regions further away from the feed [13], the gradient of the cone was optimised to improve the impedance matching at the high frequency band.

LIMITATIONS & FUTURE WORK

The difference in simulated and measured results could likely be due to discrepancies in the characteristics between the simulated and measured substrate. For instance, components were simulated to be of perfect electrical conductor (pec) material, which is an idealised material that does not exist in the real world. Surfaces like the ground plane and monocone were simulated to have zero thickness in order to ensure the mesh size was manageable enough for the software to run. The margin of error due to measurement devices, as well as feeding mismatches were also not considered in simulation. The above limitations can be further investigated.

Due to the wide impedance bandwidth, the proposed antenna has further great potential for various wireless transmission and communication systems. Although it has been devised for usage within a particular bandwidth, its characteristics can be extended to various applications, and the design parameters further investigated to optimise operation over wider bandwidths.

CONCLUSION

The proposed Ant. 2 design has met the requirements of the suggested hypothesis. It has a low profile of 16mm ($0.12\lambda_o$ at the lowest operating frequency of 2.3GHz) as compared to traditional quarter-wave ($\lambda_o/4$) monopole antennas. The simple monocone (Ant. 1) was designed to suit a higher frequency band such as UWB (3.1-10.6GHz). The shorted ring patch was then adopted to generate additional lower frequency bands, such as wireless broadband (WiBro; 2.3-2.39GHz) and wireless local area networks (WLAN; 2.4-2.484GHz). The resultant design (Ant. 2) has a wide enough bandwidth of 15.8GHz (2.2-18.0GHz) to cover a wide range of wireless services.

ACKNOWLEDGEMENTS

I would like to thank my mentors, Mr Lim Zi Wei and Dr Ang Teng Wah, as well as everyone at the DSO EN Division, for their invaluable guidance and support in this project.

REFERENCES

[1] H.-D. Chen, "Compact CPW-fed dual-frequency monopole antenna," *Electronics Letters*, vol. 38, no. 25, pp. 1622–1624, Dec. 2002.

[2] W.-C. Liu, "Broadband dual-frequency meandered CPW-fed monopole antenna," *Electronics Letters*, vol. 40, no. 21, pp. 1319–1320, Oct. 2004.

[3] W. C. Liu, "Dual wideband coplanar waveguide-fed notched antennas with asymmetrical grounds for multi-band Wireless Application," *IET Microwaves, Antennas & Propagation*, vol. 1, no. 5, pp. 980–985, Oct. 2007.

[4] H. Wang and M. Zheng, "Triple-band Wireless Local Area Network Monopole antenna," *IET Microwaves, Antennas & Propagation*, vol. 2, no. 4, pp. 367–372, Jul. 2008.

[5] C.-Y.-D. Sim, "Dual band CPW-fed monopole antenna with asymmetrical ground plane for bandwidth enhancement," *Microwave and Optical Technology Letters*, vol. 50, no. 11, pp. 3001–3004, Aug. 2008.

[6] Y. Jee and Y.-M. Seo, "Triple-band CPW-fed compact monopole antennas for GSM/pcs/DCS/WCDMA applications," *Electronics Letters*, vol. 45, no. 9, pp. 446–448, May 2009.

[7] R. Webster, "20-70 MC Monopole antennas on ground-based vehicles," *IRE Transactions on Antennas and Propagation*, vol. 5, no. 4, pp. 363–368, Oct. 1957.

[8] M. Cerretelli, V. Tesi, and G. Biffi Gentili, "Design of a shape-constrained dual-band polygonal monopole for car roof mounting," *IEEE Transactions on Vehicular Technology*, vol. 57, no. 3, pp. 1398–1403, May 2008.

[9] K. L. Lau and K. M. Luk, "A wide-band monopolar wire-patch antenna for indoor base station applications," *IEEE Antennas and Wireless Propagation Letters*, vol. 4, pp. 155–157, Jun. 2005.

[10] J.-S. Row, S.-H. Yeh, and K.-L. Wong, "A wide-band monopolar plate-patch antenna," *IEEE Transactions on Antennas and Propagation*, vol. 50, no. 9, pp. 1328–1330, Aug. 2002.

[11] J. Tak, D.-G. Kang, and J. Choi, "Stepped cylindrical antenna with a higher-order mode ring patch for wideband conical radiation pattern," *International Journal of Antennas and Propagation*, vol. 2015, pp. 1–7, May 2015.

[12] K.-L. Lau, P. Li, and K.-M. Luk, "A monopolar patch antenna with very wide impedance bandwidth," *IEEE Transactions on Antennas and Propagation*, vol. 53, no. 3, pp. 1004–1010, Mar. 2005.

[13] J. Zhao, T. Peng, C.-C. Chen, and J. Y. Volakis, "Low-profile ultra-wideband inverted-hat monopole antenna for 50 mhz–2 ghz operation," *Electronics Letters*, vol. 45, no. 3, pp. 142–144, Mar. 2009.Mar. 2009.

APPENDIX

Fig. 9: Simulated return loss for (a) shorting pin heights 11-14mm, (b) shorting pin radii 1-3mm, and (c) ring patch widths 4-6mm.

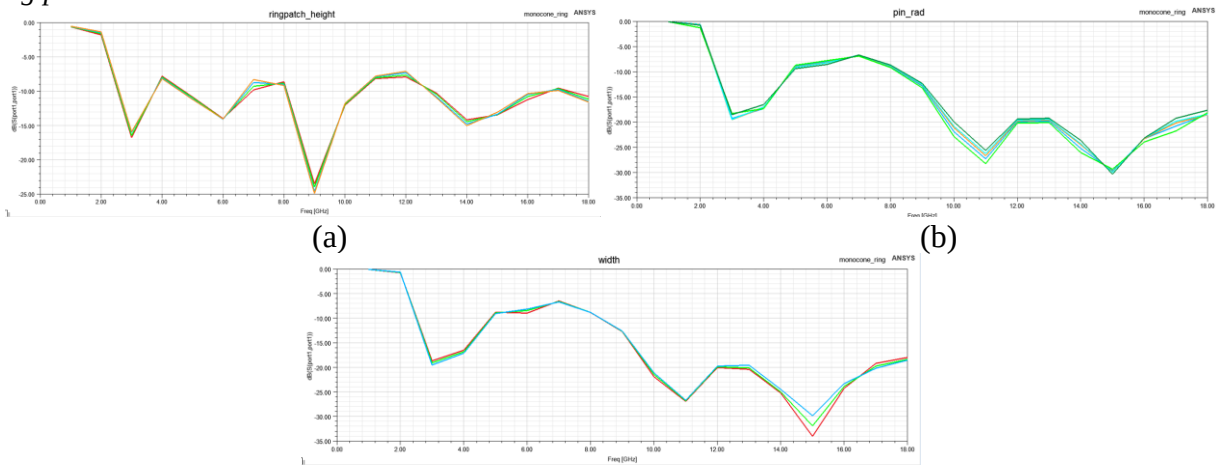

(a) (b)

(c)

Fig. 10: Simulated return loss characteristics for various (a) lr *and (b)* ur *of the monocone.*

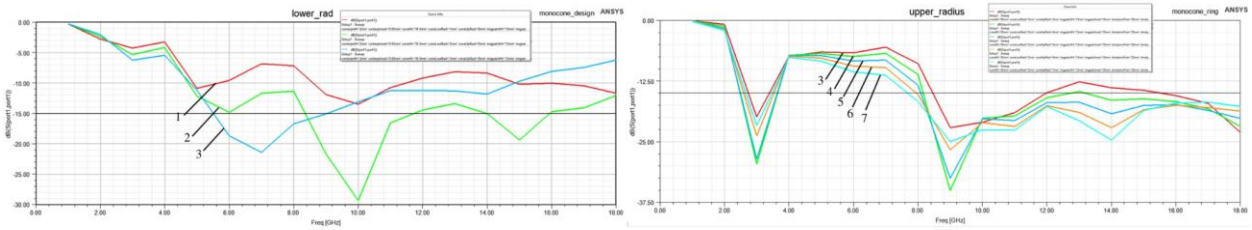

(a) (b)